Supplementary Materials for

Partisans Process Policy-Based and Identity-Based Messages using Dissociable Neural Systems

in press, Cerebral Cortex

Nir Jacoby*[1,2], Marika Landau-Wells[3], Jacob Pearl[4], Alexandra Paul[4], Emily B. Falk[4,5,6,7], Emile G. Bruneau[4], Kevin N. Ochsner[2]

1. Department of Psychological and Brain Sciences, Dartmouth College, Hanover, NH 03755.
2. Department of Psychology, Columbia University, New York, NY 10027.
3. Travers Department of Political Science, University of California-Berkeley, Berkeley, CA 94720.
4. Annenberg School for Communication, University of Pennsylvania, Philadelphia, PA 19104.
5. Wharton School, University of Pennsylvania, Philadelphia, PA 19104.
6. Department of Psychology, University of Pennsylvania, Philadelphia, PA 19104.
7. Annenberg Public Policy Center, University of Pennsylvania, Philadelphia, PA 19104

*Corresponding authors:

Nir Jacoby

nir.jacoby@dartmouth.edu

6207 Moore Hall, Dartmouth College,

Hanover, NH 03755

Kevin N. Ochsner

ko2132@columbia.edu

Department of Psychology, Columbia University, New York, NY 10027

Supplementary Information:

1. **Stimuli details and validation.**

Table S1. Details of stimuli used in the experiment.

Clip Name	Speaker	Length	Partisan orientation	Condition	Link
Support the Troops	Trae Crowder	3:05	Democratic	*Control*	https://www.youtube.com/watch?v=IIACBLGORZg&ab_channel=TraeCrowder
The girls are marching again	Chad Prather	2:22	Republican	*Control*	https://www.youtube.com/watch?v=Ar0Qw6YnVik&t=64s&ab_channel=ChadPrather
Immigration Reforms and the Economy	Robert Reich	2:57	Democratic	*Policy-Based Discourse*	https://www.youtube.com/watch?v=W6uQ6M_ybWs&t=81s&ab_channel=MoveOn
Why I Left the Left	Dave Rubin	4:22	Republican	*Policy-Based Discourse*	https://www.youtube.com/watch?v=hiVQ8vrGA_8&ab_channel=PragerU
Thanks Obama	Trae Crowder	3:17	Democratic	*Identity-Based Discourse*	https://www.youtube.com/watch?v=nM5eiunbDzQ&ab_channel=TraeCrowder
Farewell Mr. President	Chad Prather	3:22	Republican	*Identity-Based Discourse*	https://www.youtube.com/watch?v=j3DWvhXKEdI&ab_channel=ChadPrather

Video stimuli were validated by collecting data on Amazon's Mechanical Turk platform from a sample of self-identified Democrats (N = 369, including 112 leaners) and Republicans (N = 218, including 93 leaners) (Total N = 587). Each video was rated on four dimensions: bias, objectivity, reasonableness and comprehensibility (i.e. could the content be understood easily). To assess the first two dimensions, a version of the Naïve Realism Questionnaire (Pronin et al., 2002) was used to assess the extent to which participants felt the videos were biased (3 items, averaged into a Bias index) or objective (4 items, averaged into an Objectivity index). The third and fourth dimensions were assessed using ratings of reasonableness (1 item) and the extent to which participants understood the content (2 items, averaged into a Comprehension index). All analyzed items were rated on a 7-point Likert-type scale with the exception of Reasonableness, which was rated on a 0-100 point scale. Ratings were non-normally distributed. Therefore, we used a non-parametric test to compare our samples (Mann-Whitney U test).

Consistent with analyses in the study, we tested for partisan interpretation of the videos by contrasting in-party ratings (i.e., ratings provided by participants whose party identification was aligned with the speaker's partisan orientation) and out-party ratings (i.e., ratings provided by participants whose party identification did not align with the speaker's partisan orientation).

Although all videos should be rated for high levels of comprehensibility (i.e. ease of understanding the content), the goal of stimulus validation was to ensure that ratings for the other three dimensions differed between conditions as expected. Ratings of objectivity, bias, and reasonableness should not differ across control videos, regardless of whether the speaker was a Democrat or a Republican, because partisan content was not conveyed. By contrast, videos in the two discourse conditions, where speakers expressed partisan views, should seem more objective, less biased and more reasonable to participants with similar partisanship (i.e. in-party participants) as opposed to seeming less objective, more biased and less reasonable to participants with differing partisanship (i.e., out-party participants).

Analysis of M-Turk rating data validated these expectations (for tabular summary of normative ratings and statistical comparisons, see Table S2). All videos were judged to be comprehensible (median range: 5.5-6.5). For our *Control* condition videos, there were no partisan differences in the ratings for bias, objectivity, or reasonableness. In-party participants judged both *Identity-Based Discourse* condition videos to be significantly more reasonable, less biased, and more objective than out-party participants. In-party participants also judged both *Policy-Based Discourse* condition videos to be significantly more reasonable, less biased, and more objective than out-party participants.

In addition, we compared video ratings across conditions (for full comparison between conditions and statistics, see Table S3). Compared to control condition videos, participants rated *Identity-Based Discourse* condition videos as less reasonable, and less objective. Participants judged *Policy-Based Discourse* condition videos to be just as reasonable as *Control* condition videos, but also judged them to be both more objective and more influenced by biases. We interpret these differences as participants' recognition that policy positions are influenced by political and personal stances, while the video content also reflects a fact-based, data-driven argument.

Finally, participants rated *Identity-Based Discourse* videos as significantly less reasonable, less objective, and more biased than *Policy-Based Discourse* condition videos. Based on the differences within and across conditions, we concluded that videos in both of our discourse conditions were capable of activating partisan processing relative to the *Control* condition. Further, differences in reasonableness and objectivity between our *Identity-Based Discourse* and *Policy-Based Discourse* condition videos provided evidence that participants distinguished between the types of stimuli as argument-driven (*Policy-Based Discourse* condition) and not argument-driven (*Identity-Based Discourse* condition).

Table S2. Stimulus pre-testing results – all tests are two-sided Mann-Whitney U tests.

	***Control* condition**							
	Democrats aligned speaker				***Republicans aligned speaker***			
	Ingroup median	Outgroup Median	*W*	*p*	Ingroup median	Outgroup Median	*W*	*p*
Reasonableness	94	93	893.5	0.77	67	70	852.5	0.81
Comprehension Index	6.5	6.5	954	0.82	6.5	6.5	892	0.92
Bias Index	4.0	3.3	919.5	0.95	3.5	4.0	781.5	0.39
Objectivity Index	5.3	4.8	1018.5	0.44	3.6	3.0	1037.0	0.17

	***Policy-Based Discourse* condition**							
	Democrats aligned speaker				***Republicans aligned speaker***			
	Ingroup median	Outgroup Median	*W*	*p*	Ingroup median	Outgroup Median	*W*	*p*
Reasonableness	90	72	1407	0	90.5	70	2996	0.00
Comprehension Index	6.5	6.5	1050	0.366	6.5	6	1734	0.06
Bias Index	4.0	4.5	666.0	0.02	4.0	4.5	1681.5	0.04
Objectivity Index	5.8	4.1	1546.0	0.00	5.0	4.3	2893.0	0.00

	***Identity-Based Discourse* condition**							
	Democrats aligned speaker				***Republicans aligned speaker***			
	Ingroup median	Outgroup Median	*W*	*p*	Ingroup median	Outgroup Median	*W*	*p*
Reasonableness	78	32.5	1770.5	0	85	30	1494.5	0.00
Comprehension Index	6.5	5.5	1372	0.014	6	6	1083.5	0.05
Bias Index	4.7	5.7	613.5	0.00	4.7	6.3	393.5	0.00
Objectivity Index	4.0	2.3	1614.0	0.00	5.0	2.5	1449.5	0.00

Table S3. Between conditions comparison results – all tests are two-sided Mann-Whitney U tests.

***Policy-Based Discourse* condition vs *Control* condition**				
Directed effect	*Policy-Based Discourse*	*Control*	*W*	*p*
Reasonableness (Policy-Based <> Control)	81.5	81	20449	0.865
Bias Index (Poicy-Based > Control)	4.33	4	25175	<0.001
Objectivity Index (Policy-Based > Control)	4.9	4.3	24095.0	0.004

***Identity-Based Discourse* condition vs *Control* condition**				
Directed effect	*Identiy-Based Discourse*	*Control*	*W*	*p*
Reasonableness (Idnetity-Based < Control)	57	81	10292	<0.001
Bias Index (Identity-Based > Control)	5.33	4	24366	<0.001
Objectivity Index (Identity-Based < Control)	3.5	4.3	12518.0	0.001

***Policy-Based Discourse* condition vs *Identity-Based Discourse* condition**				
Directed effect	*Policy-Based Discourse*	*Identiy-Based Discourse*	*W*	*p*
Reasonableness (Policy-Baesed > Identity-Based)	81.5	57	14094	<0.001
Bias Index (Policy-Based < Identity-Based)	4.33	5.33	28485	<0.001
Objectivity Index (Policy-Based > Identity-Based)	4.9	3.5	13504.0	<0.001

2. fMRIPrep boilerplate.

Results included in this manuscript come from preprocessing performed using *fMRIPrep* 20.1.0rc3 (Esteban, Blair, et al., 2018; Esteban, Markiewicz, et al., 2018; RRID:SCR_016216), which is based on *Nipype* 1.4.2 (K. Gorgolewski et al., 2011; K. J. Gorgolewski et al., 2018; RRID:SCR_002502).

Anatomical data preprocessing

The T1-weighted (T1w) image was corrected for intensity non-uniformity (INU) with N4BiasFieldCorrection (Tustison et al., 2010), distributed with ANTs 2.2.0 (Avants et al., 2008, RRID:SCR_004757), and used as T1w-reference throughout the workflow. The T1w-reference was then skull-stripped with a Nipype implementation of the antsBrainExtraction.sh workflow (from ANTs), using OASIS30ANTs as target template. Brain tissue segmentation of cerebrospinal fluid (CSF), white-matter (WM) and gray-matter (GM) was performed on the brain-extracted T1w using fast (FSL 5.0.9, RRID:SCR_002823, Zhang et al., 2001). Brain surfaces were reconstructed using recon-all (FreeSurfer 6.0.1, RRID:SCR_001847, Dale et al., 1999), and the brain mask estimated previously was refined with a custom variation of the method to reconcile ANTs-derived and FreeSurfer-derived segmentations of the cortical gray-matter of Mindboggle (RRID:SCR_002438, Klein et al., 2017). Volume-based spatial normalization to one standard space (MNI152NLin2009cAsym) was performed through nonlinear registration with antsRegistration (ANTs 2.2.0), using brain-extracted versions of both T1w reference and the T1w template. The following template was selected for spatial normalization: ICBM 152 Nonlinear Asymmetrical template version 2009c (Fonov et al., 2009, RRID:SCR_008796; TemplateFlow ID: MNI152NLin2009cAsym).

Functional data preprocessing

For each of the functional runs found per subject (across all tasks and sessions), the following preprocessing was performed. First, a reference volume and its skull-stripped version were generated using a custom methodology of fMRIPrep. Head-motion parameters with respect to the BOLD reference (transformation matrices, and six corresponding rotation and translation parameters) are estimated before any spatiotemporal filtering using mcflirt (FSL 5.0.9, Jenkinson et al., 2002). Susceptibility distortion correction (SDC) was omitted. The BOLD reference was then co-registered to the T1w reference using bbregister (FreeSurfer) which implements boundary-based registration (Greve & Fischl, 2009). Co-registration was configured with six degrees of freedom. The BOLD time-series (including slice-timing correction when applied) were resampled onto their original, native space by applying the transforms to correct for head-motion. These resampled BOLD time-series will be referred to as preprocessed BOLD in original space, or just preprocessed BOLD. The BOLD time-series were resampled into standard space, generating a preprocessed BOLD run in MNI152NLin2009cAsym space. First, a reference volume and its skull-stripped version were generated using a custom methodology of fMRIPrep. Several confounding time-series were calculated based on the preprocessed BOLD: framewise displacement (FD), DVARS and three region-wise global signals. FD was computed using two formulations following Power (absolute sum of relative motions, Power et al., 2014)) and Jenkinson (relative root mean square displacement between affines, Jenkinson et al., 2002)). FD and DVARS are calculated for each functional run, both using their implementations in Nipype (following the definitions by Power et al., 2014). The three global signals are extracted within the CSF, the WM, and the whole-brain masks. Additionally, a set of physiological regressors were extracted to allow for component-based noise correction (CompCor, Behzadi et al., 2007). Principal components are estimated after high-pass filtering the preprocessed BOLD time-series (using a discrete cosine filter with 128s cut-off) for the two CompCor variants: temporal (tCompCor) and anatomical (aCompCor). tCompCor components are then calculated from the top 5% variable voxels within a mask covering the subcortical regions. This subcortical mask is obtained by heavily eroding the brain mask, which ensures it does not include cortical GM regions. For aCompCor, components are calculated within the intersection of the aforementioned mask and the union of CSF and WM masks calculated in T1w space, after their projection to the native space of each functional run (using the inverse BOLD-to-T1w transformation). Components are also calculated separately within the WM and CSF masks. For each CompCor decomposition, the k components with the largest singular values are retained, such that the retained components' time series are sufficient to explain 50 percent of variance across the nuisance mask (CSF, WM, combined, or temporal). The remaining components are dropped from consideration. The head-motion estimates calculated in the correction step were also placed within the corresponding confounds file. The confound time series derived from head motion estimates and global signals were expanded with the inclusion of temporal derivatives and quadratic terms for each (Satterthwaite et al., 2013). Frames that exceeded a threshold of 0.5 mm FD or 1.5 standardised DVARS were annotated as motion outliers. All resamplings can be performed with a single interpolation step by composing all the pertinent transformations (i.e. head-motion transform

matrices, susceptibility distortion correction when available, and co-registrations to anatomical and output spaces). Gridded (volumetric) resamplings were performed using antsApplyTransforms (ANTs), configured with Lanczos interpolation to minimize the smoothing effects of other kernels (Lanczos, 1964). Non-gridded (surface) resamplings were performed using mri_vol2surf (FreeSurfer).
Many internal operations of fMRIPrep use Nilearn 0.6.2 (Abraham et al., 2014, RRID:SCR_001362), mostly within the functional processing workflow. For more details of the pipeline, see the section corresponding to workflows in fMRIPrep's documentation.

3. Functional localizers comparison.

Prior literature found that the activation in the Socio-political reasoning localizer task generate a brain pattern that looks similar to the mentalizing localizer (False-belief) task (Bruneau & Saxe, 2010). For visual comparison between the localizers, we ran a second level (group) analysis on the results of both functional localizer tasks (Figure S1). The analysis was done as a one sample t-test across participants in each of the tasks. Correction for multiple comparisons was done using SnPM13 (http://www2.warwick.ac.uk/snpm) voxel-cluster correction, with θ = 0.5 (Hayasaka & Nichols, 2004)

After replicating this observation, we wanted to test whether this result is driven by a shared representation in the same voxels or by neighboring but distinct sub-populations at the individual level (DiNicola et al., 2020; Scholz et al., 2009). To test that we compared the fROIs picked by the two tasks at the individual level. First, we tested the precent of overlapping voxels within each region (out of the fixed number of voxels picked. Second, for each successfully picked fROI we calcultated the center of mass (in MNI coordinates) and then compared across participants whether there was a consistent difference in the center of mass between the loci of both tasks. This was done using a paired Hotelling's T2 test (Hotelling, 1992) which is a multi-dimensional generalization of a t-test (Table S4).

Table S4. Functional localizers comparison at the participant level.

Region	N subs	overlapping voxels	% overlap	Hotelling's *T2*		
DMPFC	49	15.71 / 92	17.1%	$T2$ = 6.64	$F(3,46)$ = 2.12	p = 0.11
LTPJ	52	26.81 / 172	15.6%	$T2$ = 67.07	$F(3,49)$ = 21.48	p << 0.001
MMPFC	51	10.49 / 81	13.0%	$T2$ = 11.92	$F(3,48)$ = 3.81	p = 0.016
PC	52	24.06 / 195	12.3%	$T2$ = 40.06	$F(3,49)$ = 12.83	p << 0.001
RSTS	51	27.8 / 192	14.5%	$T2$ = 21.74	$F(3,48)$ = 6.96	p < 0.001
RTPJ	52	23.48 / 175	13.4%	$T2$ = 97.04	$F(3,49)$ = 31.08	p << 0.001
VMPFC	50	8.1 / 59	13.7%	$T2$ = 9.8	$F(3,47)$ = 3.13	p = 0.034

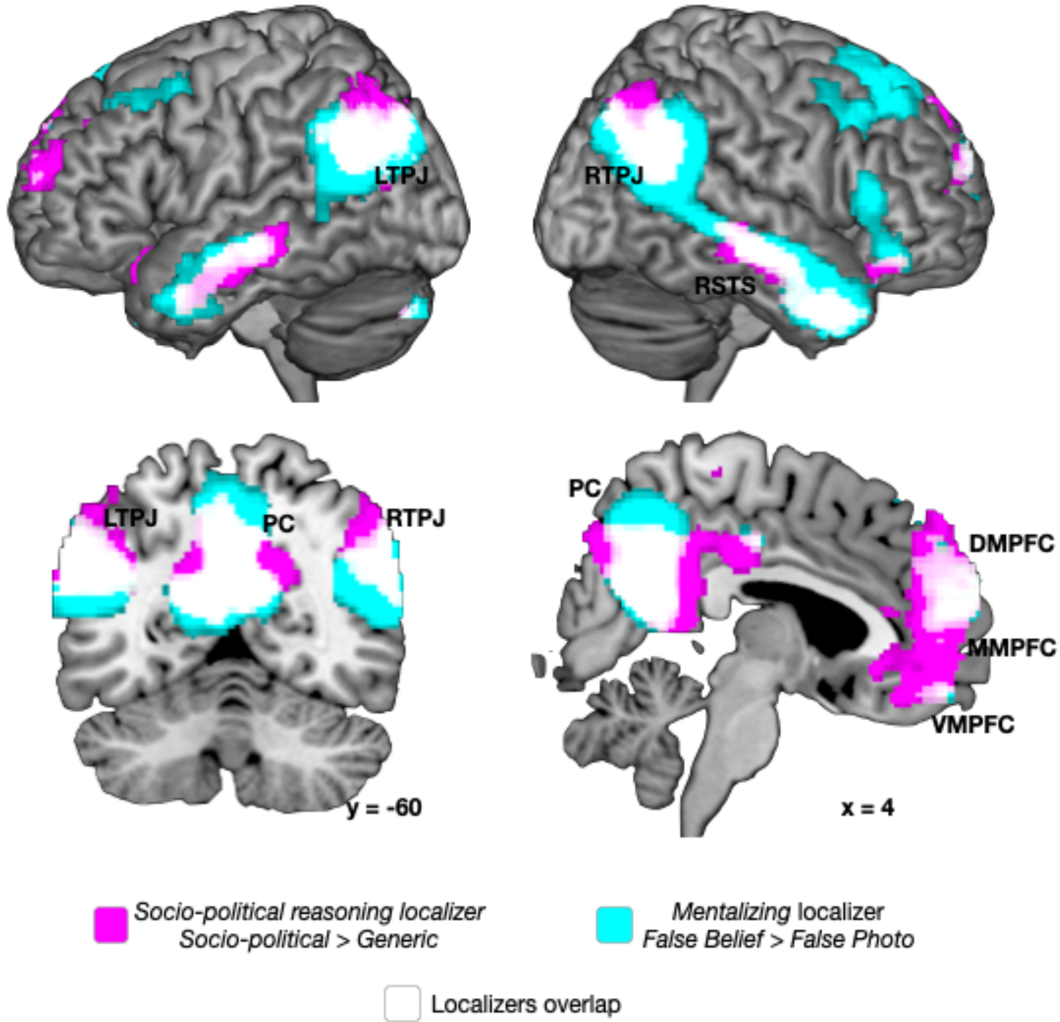

Fig. S1. Functional localizers comparison at the group-level: Whole-brain analysis ($p < 0.05$ corrected). Abbreviations: D/M/VMPFC, dorsal/middle/venttal medial prefrontal cortex; RSTS, right superior temporal sulcus; L/RTPJ, left/right temporoparietal junction; PC, precuneus.

SI References

Abraham, A., Pedregosa, F., Eickenberg, M., Gervais, P., Mueller, A., Kossaifi, J., Gramfort, A., Thirion, B., & Varoquaux, G. (2014). Machine learning for neuroimaging with scikit-learn. *Frontiers in Neuroinformatics*, *8*, 14. https://doi.org/10.3389/fninf.2014.00014

Avants, B. B., Epstein, C. L., Grossman, M., & Gee, J. C. (2008). Symmetric diffeomorphic image registration with cross-correlation: Evaluating automated labeling of elderly and neurodegenerative brain. *Medical Image Analysis*, *12*(1), 26–41. https://doi.org/10.1016/j.media.2007.06.004

Behzadi, Y., Restom, K., Liau, J., & Liu, T. T. (2007). A component based noise correction method (CompCor) for BOLD and perfusion based fMRI. *NeuroImage*, *37*(1), 90–101. https://doi.org/10.1016/j.neuroimage.2007.04.042

Bruneau, E. G., & Saxe, R. (2010). Attitudes towards the outgroup are predicted by activity in the precuneus in Arabs and Israelis. *NeuroImage*, *52*(4), 1704–1711. https://doi.org/10.1016/j.neuroimage.2010.05.057

Dale, A. M., Fischl, B., & Sereno, M. I. (1999). Cortical surface-based analysis. I. Segmentation and surface reconstruction. *NeuroImage*, *9*(2), 179–194. https://doi.org/10.1006/nimg.1998.0395

DiNicola, L. M., Braga, R. M., & Buckner, R. L. (2020). Parallel distributed networks dissociate episodic and social functions within the individual. *Journal of Neurophysiology*, *123*(3), 1144–1179. https://doi.org/10.1152/jn.00529.2019

Esteban, O., Blair, R., Markiewicz, C. J., Berleant, S. L., Moodie, C., Ma, F., Isik, A. I., Erramuzpe, A., Kent, J. D., Goncalves, M., DuPre, E., Sitek, K. R., Gomez, D. E. P., Lurie, D. J., Ye, Z., Salo, T., Valabregue, R., Amlien, I. K., Liem, F., … Gorgolewski, K. J. (2018). *FMRIPrep software* [Computer software]. Zenodo. https://doi.org/10.5281/zenodo.852659

Esteban, O., Markiewicz, C. J., Blair, R. W., Moodie, C. A., Isik, A. I., Erramuzpe, A., Kent, J. D., Goncalves, M., DuPre, E., Snyder, M., Oya, H., Ghosh, S. S., Wright, J., Durnez, J., Poldrack, R. A., & Gorgolewski, K. J. (2018). fMRIPrep: A robust preprocessing pipeline for functional MRI. *Nature Methods*, *16*(1), 1–14. https://doi.org/10.1038/s41592-018-0235-4

Fonov, V. S., Evans, A. C., McKinstry, R. C., Almli, C. R., & Collins, D. L. (2009). Unbiased nonlinear average age-appropriate brain templates from birth to adulthood. *NeuroImage*, *47*(S1), S102. https://doi.org/10.1016/S1053-8119(09)70884-5

Gorgolewski, K., Burns, C. D., Madison, C., Clark, D., Halchenko, Y. O., Waskom, M. L., & Ghosh, S. S. (2011). Nipype: A flexible, lightweight and extensible neuroimaging data processing framework in python. *Frontiers in Neuroinformatics*, *5*, 13. https://doi.org/10.3389/fninf.2011.00013

Gorgolewski, K. J., Esteban, O., Markiewicz, C. J., Ziegler, E., Ellis, D. G., Jarecka, D., Notter, M. P., Johnson, H., Burns, C., Manhães-Savio, A., Hamalainen, C., Yvernault, B., Salo, T., Goncalves, M., Jordan, K., Waskom, M., Wong, J., Modat, M., Loney, F., … Ghosh, S. (2018). *Nipype Software* [Computer software]. Zenodo. https://zenodo.org/record/596855

Greve, D. N., & Fischl, B. (2009). Accurate and robust brain image alignment using boundary-based registration. *NeuroImage*, *48*(1), 63–72. https://doi.org/10.1016/j.neuroimage.2009.06.060

Hayasaka, S., & Nichols, T. E. (2004). Combining voxel intensity and cluster extent with permutation test framework. *NeuroImage*, *23*(1), 54–63. https://doi.org/10.1016/j.neuroimage.2004.04.035

Hotelling, H. (1992). The generalization of Student's ratio. In *Breakthroughs in statistics* (pp. 54–65). Springer.

Jenkinson, M., Bannister, P., Brady, M., & Smith, S. (2002). Improved Optimization for the Robust and Accurate Linear Registration and Motion Correction of Brain Images. *NeuroImage*, *17*(2), 825–841. https://doi.org/10.1006/nimg.2002.1132

Klein, A., Ghosh, S. S., Bao, F. S., Giard, J., Häme, Y., Stavsky, E., Lee, N., Rossa, B., Reuter, M., Chaibub Neto, E., & Keshavan, A. (2017). Mindboggling morphometry of human brains. *PLOS Computational Biology*, *13*(2), e1005350-40. https://doi.org/10.1371/journal.pcbi.1005350

Lanczos, C. (1964). Evaluation of Noisy Data. *Journal of the Society for Industrial and Applied Mathematics: Series B, Numerical Analysis*, *1*, 76–85. https://doi.org/10.2307/2949766?refreqid=search-gateway:364f31072117b0bc53d3b01674385517

Power, J. D., Mitra, A., Laumann, T. O., Snyder, A. Z., Schlaggar, B. L., & Petersen, S. E. (2014). Methods to detect, characterize, and remove motion artifact in resting state fMRI. *NeuroImage*, *84*(C), 320–341. https://doi.org/10.1016/j.neuroimage.2013.08.048

Pronin, E., Lin, D. Y., & Ross, L. (2002). The Bias Blind Spot: Perceptions of Bias in Self Versus Others. *Personality and Social Psychology Bulletin*, *28*(3), 369–381. https://doi.org/10.1177/0146167202286008

Satterthwaite, T. D., Elliott, M. A., Gerraty, R. T., Ruparel, K., Loughead, J., Calkins, M. E., Eickhoff, S. B., Hakonarson, H., Gur, R. C., Gur, R. E., & Wolf, D. H. (2013). An improved framework for confound regression and filtering for control of motion artifact in the preprocessing of resting-state functional connectivity data. *NeuroImage*, *64*, 240–256. https://doi.org/10.1016/j.neuroimage.2012.08.052

Scholz, J., Triantafyllou, C., Whitfield-Gabrieli, S., Brown, E. N., & Saxe, R. (2009). Distinct regions of right temporo-parietal junction are selective for theory of mind and exogenous attention. *PLoS ONE*, *4*(3), e4869. https://doi.org/10.1371/journal.pone.0004869

Tustison, N. J., Avants, B. B., Cook, P. A., Yuanjie Zheng, Egan, A., Yushkevich, P. A., & Gee, J. C. (2010). N4ITK: Improved N3 Bias Correction. *IEEE Transactions on Medical Imaging*, *29*(6), 1310–1320. https://doi.org/10.1109/TMI.2010.2046908

Zhang, Y., Brady, M., & Smith, S. (2001). Segmentation of brain MR images through a hidden Markov random field model and the expectation-maximization algorithm. *IEEE Transactions on Medical Imaging*, *20*(1), 45–57. https://doi.org/10.1109/42.906424